Solar Physics
DOI: 10.1007/•••••-•••-•••-••••-•

Study of Forbush Decrease Recovery Times by the *Payload for Antimatter Matter Exploration and Light-nuclei Astrophysics* (PAMELA) Experiment

I. Lagoida[1] · S. Voronov[1] · V. Mikhailov[1] · M. Boezio[2] · R. Munini[2] · G. Barbarino[3,4] · G. Bazilevskaya[5] · R. Bellotti[6,7] · A. Bogomolov[8] · V. Bonvicini[2] · F. Cafagna[6,7] · D. Campana[4] · M. Casolino[9,10] · A. Galper[1] · S. Koldobskiy[11] · A. Kvashnin[5] · A. Lenni[2] · A. Leonov[1] · V. Malakhov[1] · L. Marcelli[12] · N. Marcelli[9] · M. Martucci[12,13] · A. Mayorov[1] · M. Mergè[9,12] · E. Mocchiutti[2] · A. Monaco[3,7] · B. Panico[4] · P. Picozza[9,12] · M. Ricci[13] · S. B. Ricciarini[14] · S. Rodenko[1] · A. Sotgiu[12] · R. Sparvoli[12,9] · Y. Stozhkov[5] · A. Vacchi[2,15] · E. Vannuccini[4] · G. Vasilyev[8] · Y. Yurkin[1] · G. Zampa[2] · N. Zampa[2]

✉ I.A. Lagoida
ialagoida@mephi.ru

[1] National Research Nuclear University MEPhI, RU-115409, Moscow, Russia

[2] INFN, Sezione di Trieste, I-34149 Trieste, Italy

[3] University of Naples "Federico II," Department of Physics, I-80126 Naples, Italy

[4] INFN, Sezione di Naples, I-80126 Naples, Italy

[5] Lebedev Physical Institute, RU-119991, Moscow, Russia

[6] University of Bari, Department of Physics, I-70126 Bari, Italy

[7] INFN, Sezione di Bari, I-70126 Bari, Italy

[8] Ioffe Physical Technical Institute, RU-194021 St. Petersburg, Russia

[9] INFN, Sezione di Rome "Tor Vergata," I-00133 Rome, Italy

[10] RIKEN, Advanced Science Institute, Wako-shi, Saitama, Japan

Abstract A Forbush decrease (FD) is a sudden drop of cosmic ray intensity arising as an effect of coronal mass ejection (CME) propagation in interplanetary space. The different physical properties of each CME cause variability in the FDs observed by scientific instruments. A comprehensive study of both phenomena is required to properly understand the processes involved in FDs. Most of the current studies in this field use experimental data obtained by ground-based apparatus that measure the flux of cosmic rays via their interaction with Earth's atmosphere. Direct measurements in space of FDs are rather rare. In this work, we present the results obtained by the spacecraft-borne experiment *Payload for Antimatter Matter Exploration and Light-nuclei Astrophysics* (PAMELA). The experiment took data from 15 June 2016 until January 2016. A Series of FDs during the period 2006 – 2013 were studied. Only significant events with amplitude $\geq 10\,\%$ for the proton flux $R = 1.1 - 2.9\,\mathrm{GV}$ were taken into account. The dependencies of the recovery times on the particle rigidity were obtained for FD events generated by halo-type CMEs.

Keywords: Cosmic Rays, Coronal Mass Ejections

1. Introduction

Forbush (1937) measured a sharp decline in cosmic ray intensity. This phenomenon, named the Forbush decrease (FD), became a popular scientific topic in low-energy cosmic ray physics. Despite several decades of FD studies, there is still no clear understanding of the main mechanism responsible for this effect.

Nowadays, it is believed that the source of this phenomenon is associated with coronal mass ejections (CMEs) from the Sun's surface. This magnetized coronal plasma then propagates through the heliosphere becoming what is known as an interplanetary coronal mass ejection (ICME) (e.g. Lockwood, 1971; Wibberenz *et al.*, 1998; Cane, 2000; Gopalswamy, 2006; Nieves-Chinchilla *et al.*, 2018).

A classical ICME consists of three stages: a shock-wave, a sheath region, and an ejecta part. A shock-wave is the high-speed part of an ICME produced by the explosive nature of the CME. This stage is characterized by sudden increases in the interplanetary magnetic field and in the speed of the solar-wind. The sheath region is produced by the shock and is characterized by a highly disturbed interplanetary medium, which in turn results in enhanced fluctuations of the magnetic field and solar-wind speed. The third stage is the passage of the

[11] Space Physics and Astronomy Research Unit and Sodankylä Geophysical Observatory, University of Oulu, Finland

[12] University of Rome "Tor Vergata," Department of Physics, I-00133 Rome, Italy

[13] INFN, Laboratori Nazionali di Frascati, Via Enrico Fermi 40, I-00044 Frascati, Italy

[14] IFAC, I-50019 Sesto Fiorentino, Florence, Italy

ejected material, which is associated with quiet periods and increased values of both the heliospheric magnetic field and the speed of the solar-wind.

The physical properties of the ICME determine the characteristics of the FD that, however, depends significantly also on where the experimental measurement takes place. Figure 1 shows solar-wind and interplanetary magnetic field data along with the proton flux measured between 1.1 and 2.9 GV by the *Payload for Antimatter Matter Exploration and Light-nuclei Astrophysics* (PAMELA) experiment in the proximity of the 14 July 2012 FD. The effect of the three stages of an ICME can be clearly observed on these parameters. According to the *Wind* spacecraft data (wind.nasa.gov/ICME_catalog), the ICME responsible for the generation of the observed FD passed the Lagrangian point [L^1] on 14 July 2012 at 17:39 UTC with the shock wave at the leading edge. By studying the temporal profiles of the proton plasma temperature [T^p], solar-wind speed [V^{sw}], and interplanetary magnetic field [$|B|$] the ICME stages can be identified. These data were obtained using the OMNI database (omniweb.gsfc.nasa.gov). The shock-wave (Stage I) manifests itself as sudden increases in the magnetic field and the solar-wind speed. The passage of the shock-wave creates a highly disturbed interplanetary medium, which is named the sheath region (Stage II). The difference between the real (T^{real}, solid line in Figure 1, Panel d) and the expected (T^{exp}, dashed line in Figure 1, Panel d) proton plasma temperature is one of the signatures of the ejecta passage (see Zurbuchen and Richardson, 2006). The expected plasma temperature is calculated using the empirical correlation of the proton plasma temperature with the solar-wind speed described in Richardson and Cane, 1995. When the ejecta moves into the region of observation the ratio T^{real} / T^{exp} becomes smaller than 0.5.

The angular width of the shock-wave is usually larger than that for the ejecta part, so FD can be generated separately by both the shock-wave and the ejecta part. On top of these dependencies, the characteristics of the FD also depend on the internal power of the ICME and its propagation properties. The interplanetary medium swept by the ICME affects the amplitude of the FDs (Belov *et al.*, 2001; Dumbović *et al.*, 2012; Alania *et al.*, 2013; Arunbabu *et al.*, 2015; Lagoida, Voronov, and Mikhailov, 2019). Furthermore, faster CMEs appear to create stronger FDs (Penna and Quillen, 2005).

Previously, contradictory results were obtained about the dependence of the FD recovery time on the rigidity of the particles. A few research groups found that the recovery time did not depend on the rigidity of the cosmic ray particles (Lockwood, Webber, and Jokipii, 1986), and concluded that the recovery time depended only on the ICME dissipation. Conversely, other groups found both types of FDs with and without dependence of their recovery time on rigidity (Usoskin *et al.*, 2008; Zhao and Zhang, 2016). All of these results were obtained using data collected by ground-based neutron monitors and muon hodoscopes. Direct measurements of cosmic ray variability during FDs performed by the space-borne PAMELA (Munini *et al.*, 2018) and *Dark Matter Particle Explore* (DAMPE) (Alemanno *et al.*, 2021) experiments revealed a clear dependence of the FD recovery time generated by fast ($\geq 1000\,\mathrm{km\,s^{-1}}$ near the Sun) ICME.

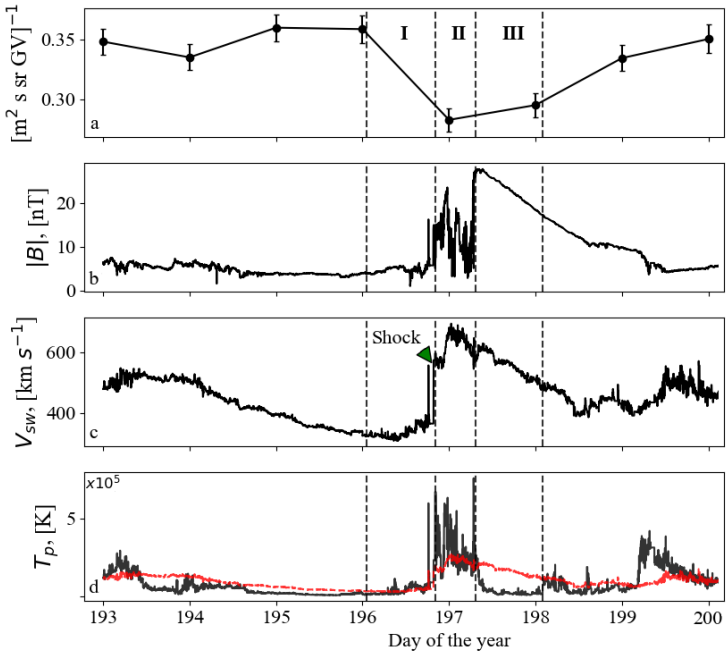

Figure 1. A FD observed in the proton flux (1.1 – 2.9 GV) measured by PAMELA on 14 July 2012 and corresponding signatures of ICME stages (I – shock-wave, II – sheath region, III – ejecta) interplanetary space features. **a** – proton flux, **b** – interplanetary magnetic field, **c** – solar-wind speed, **d** – real (*solid*), and expected (*dashed*) proton plasma temperatures.

2. Experiment

The PAMELA spacecraft instrument was designed to study the fluxes of cosmic ray p^+, p^-, e^+, e^- as well as fluxes of cosmic ray nuclei with $Z \leq 8$ in the energy range from about one hundred MeV n^{-1} to several hundred GeV n^{-1} (Picozza *et al.*, 2007; Adriani *et al.*, 2014, 2017). The PAMELA instrument comprised a time-of-flight (ToF) system, a magnetic spectrometer, an anticoincidence system, an electromagnetic calorimeter, and a neutron detector (see Figure 2). The ToF system consisted of three-segmented scintillator planes (S1, S2, and S3) divided into strips and was used to trigger the instrument and measure the ionization losses and velocities of particles. The magnetic spectrometer consisted of a permanent magnet made of an Nd-Fe-B alloy (with a residual magnetization of 1.3 T), and a microstrip silicon tracking system composed of six equidistant planes with a thickness of 300 microns. The magnetic spectrometer measured the rigidity ($R = pc/Ze$) and the charge of particles crossing the detector. The PAMELA instrument was installed onboard the Resurs – DK1 spacecraft, which was launched into low-Earth orbit on 15 June 2006 from the Baikonur Cosmodrome (Kazakhstan). Data-taking continued until January 2016.

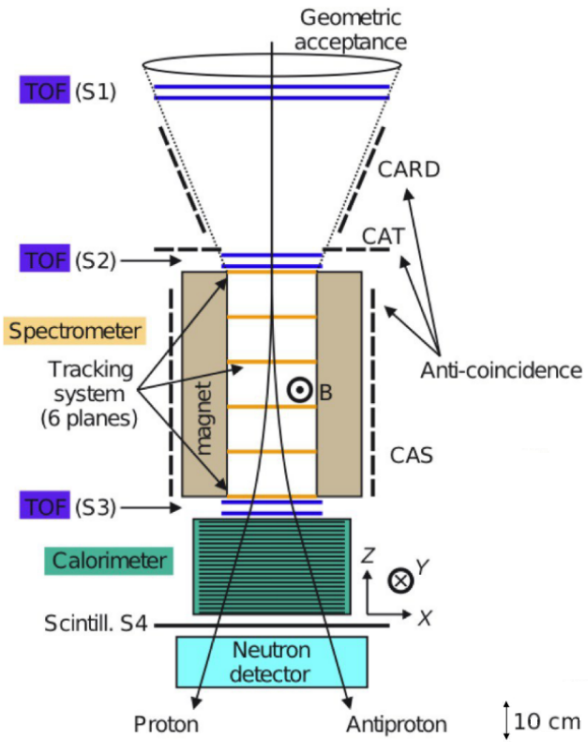

Figure 2. Schematic view of the PAMELA telescope.

3. Data Analysis and Results

The analysis was based on the daily proton fluxes measured by the PAMELA instrument in the rigidity range from 0.7 to 19 GV. The proton analysis used in this work was identical to the one presented and discussed by Martucci *et al.*, 2018.

CME candidates responsible for selected FDs were chosen using the *Solar and Heliospheric Observatory* (SOHO) CME catalog (cdaw.gsfc.nasa.gov/CME_list). Several conditions were used to select CMEs and related FDs. Only halo CMEs with an angular width of 360° were included in the selected sample to remove FDs generated by an incomplete ICME structure spreading in the vicinity of the Earth. This minimized the modulation of the FD recovery time due to the geometrical properties of the moving ICME in interplanetary space. The arrival times of the shock waves obtained by the *Wind* spacecraft were used to calculate the time of the ICME passage through the Sun – Earth region. ICMEs, and the corresponding FDs, that did not generate shock waves at the Lagrangian point [L^1] were not used. This guaranteed the choice of ICMEs with complete structures in close proximity to the Earth. The selected CMEs (ICMEs) and corresponding FDs along with the associated data are presented in Table 1, where:

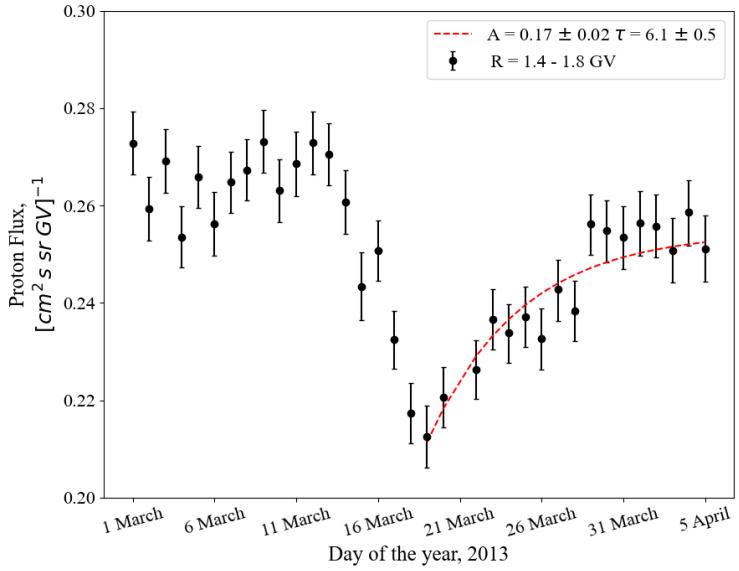

Figure 3. The temporal profile of the proton flux ($R = 1.4-1.8$ GV) measured by PAMELA experiment during 17 March 2013 FD. $\tau = 6.1$ days is the recovery time fitted with Equation 1.

t^S	start time of the CME observed by SOHO spacecraft [UTC]
t^E	start time of the ICME observed by *Wind* spacecraft [UTC]
$V^{20R_\odot}$	velocity of CME at distance of 20 solar radii [km s^{-1}]
τ^{SE}	transit time of ICME between Sun – Earth region [days]
t^{FD}	the date of FD at Earth [UTC]
A^{PAM}	FD amplitude [%] calculated for the cosmic ray proton flux measured by PAMELA experiment between 1.1 and 2.9 GV
A^{Oulu}	FD amplitude [%] calculated for cosmic rays estimated using Oulu neutron monitor daily data

The temporal profiles of FDs measured by PAMELA experiment over seven rigidity intervals (Table 2) were used to determine the FD recovery times and their possible correlation with ICME features. One of these profiles for the proton flux in the rigidity interval from 1.4 to 1.8 GV is shown in Figure 3.

The temporal profiles of each rigidity interval for the selected FDs were fitted with the following exponential function:

$$\delta I = \frac{I_0 - I}{I_0} = A \exp(\frac{t_0 - t}{\tau}) \quad (1)$$

where I and I_0 are the current and undisturbed cosmic ray intensities, correspondingly, and A is the amplitude of FD for the selected rigidity range, t_0 is the start time of FD and τ is the recovery time of FD in days. The undisturbed cosmic ray intensity was calculated as the average proton flux over four days after the end of the corresponding FD. The resulting recovery times showed different

Table 1. A sample of Forbush decreases and the corresponding properties of CMEs (ICMEs).

t^S [UTC]	t^E [UTC]	$V^{20R_\odot}$ [$km\,s^{-1}$]	τ^{SE} [$days$]	t^{FD} [UTC]	A^{PAM} [%]	A^{Oulu} [%]
13 Dec. 2006 02:54	14 Dec. 2006 13:51	1573	1.5	16 Dec. 2006	31	9
14 Dec. 2006 22:30	16 Dec. 2006 17:34	1041	1.8			
14 Feb. 2011 18:24	18 Feb. 2011 19:50	449	4	18 Feb. 2011	9.5	3
15 Feb. 2011 02:24		471	3.7			
22 Oct. 2011 01:25	24 Oct. 2011 19:50	663	2.8	24 Oct. 2011	9.4	3.1
22 Oct. 2011 10:24		1074	2.4			
23 Feb. 2012 08:12	26 Feb. 2012 20:59	562	3.5	26 Feb. 2012	10.5	2
24 Feb. 2012 03:46		874	2.7			
07 Mar. 2012 00:24	08 Mar. 2012 10:32	2594	1.4	08 Mar. 2012	33	10
07 Mar. 2012 01:30		1260	1.4			
10 Mar. 2012 18:00	12 Mar. 2012 08:28	1261	1.6			
13 Mar. 2012 17:36	15 Mar. 2012 12:35	1987	1.8			
02 Sep. 2012 04:00	04 Sep. 2012 22:02	430	2.8	04 Sep. 2012	12	5
27 Sep. 2012 10:12	30 Sep. 2012 10:14	1309	3	30 Sep. 2012	9.4	2
28 Sep. 2012 00:12		817	2.4			
28 Sep. 2012 10:36		638	2			
27 Oct. 2012 16:48	31 Oct. 2012 14:28	483	3.9	31 Oct. 2012	8	2
28 Oct. 2012 08:48		475	3.2			
15 Mar. 2013 07:12	17 Mar. 2013 05:21	1161	1.9	17 Mar. 2013	20	5
11 Apr. 2013 11:12	13 Apr. 2013 22:13	819	2.5	13 Apr. 2013	13	4

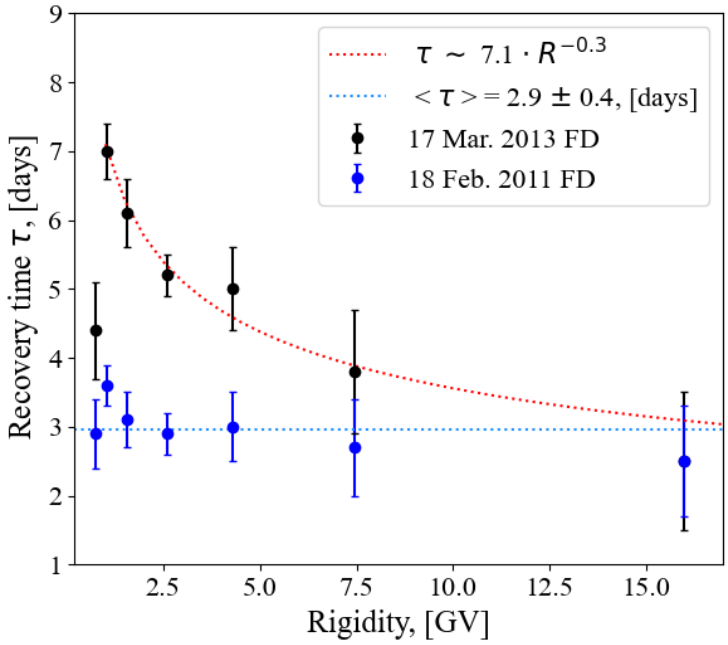

Figure 4. The dependencies of the recovery times on rigidity for FD events 18 February 2011 and 17 March 2013. The *dashed red curve* is a power-low fit of the 17 March 2013 data, the χ^2_f of this fit is equal to 0.1. The *dashed blue line* is a constant fit of the recovery times of the 18 February 2011 event. The first rigidity interval (0.69 – 0.81 GV) was not used for the fits because of the possible contribution of solar energetic particle (SEP) events.

behavior for different FD events. All the selected FDs can be divided into two types: Type I events with a clearly rigidity-dependent recovery time, Type II events with no significant rigidity-dependent recovery time. As an example, the recovery times measured in various rigidity ranges for the 18 February 2011 and 17 March 2013 FDs are shown in Figure 4 and Table 2. It can be noted that, accounting for the uncertainties, the recovery time is the same (average value: 2.9 ± 0.4 days, $\chi^2 = 10$ with dof = 5) in all the rigidity intervals for the 18 February 2011 event. Instead, the recovery times of the 17 March 2013 event have an obvious dependence on the rigidity with a χ^2 test of independence value of at $\chi^2 = 19$ (dof = 5).

4. Discussion

As shown, the FDs measured by PAMELA experiment appeared consisting of two types: having recovery time with significant (Type I) or non-significant (Type II) rigidity dependence. Moreover, the Type II FDs were characterized by an average recovery time of 2 – 3 days, while Type I FDs had larger recovery times of about 6 days. We studied if this characterization of FD events was correlated with specific features of the corresponding CMEs. Figure 5 shows the FD amplitudes

Table 2. The recovery times [days] for observed FDs. Rigidity intervals, GV: I: 0.69 – 0.8, II: 0.95 – 1.11 III: 1.37 – 1.76 IV: 2.27 – 2.92 V: 3.75 – 4.83 VI: 6.22 – 8.68 VII: 12.87 – 19.07

Date	Recovery time for each rigidity interval						
	I	II	III	IV	V	VI	VII
16 Dec. 2006	6.2	7.1	7.8	6.1	5.9	3.8	3.2
18 Feb. 2011	2.9	3.5	3.1	2.9	2.8	2.9	2.7
24 Oct. 2011	2	2.1	2	2	1.9	1.5	1.5
26 Feb. 2012	2.1	2	2	1.8	1.9	1.7	1.4
08 Mar. 2012	3.5	5.7	5.5	5.1	4.5	3.6	2.8
04 Sep. 2012	2.8	3.5	3.2	3.3	3	2.5	2.7
30 Sep. 2012	2.2	2	2	1.7	1.5	1.4	1.5
31 Oct. 2012	2.2	2.4	2	1.6	1.7	1.5	1.5
17 Mar. 2013	4.4	6.9	6.1	5.2	5	3.8	2.5
13 Apr. 2013	2.8	3	3.2	3.3	3.5	3.2	2.7

of cosmic ray proton fluxes measured by PAMELA between 1.1 and 2.9 GV versus the ICME transit times.

A clear relation between FD amplitude values and ICME transit times is observed. Furthermore, slow ICMEs (τ^{SE} > two days) are related to rigidity independent recovery time (Type II FDs, blues crosses) while fast ICMEs are related to Type I FDs (red stars). A similar relation is observed comparing the FD amplitude and the ICME propagation speed at the distance of 20 solar radii ($V^{20R_\odot}$) as shown in Figure 6.

It appears from Figures 4, 5, and 6 that faster ICMEs generate FD with large amplitude and with recovery times depending on particle rigidity. A possible explanation for this dependence is related to the process of shock-wave dissipation. When a shock-wave propagates in the interplanetary space, it sweeps particles away, causing the first rapid intensity drop of the FD. This acts differently on particles with different rigidity, affecting more low-rigidity particles. Thus, contributing to the observed difference in recovery times between high and low rigidity particles. The magnitude of this effect depends on the power of the shock-wave and its velocity. Therefore, it is significant only for powerful events for which FD amplitude $\geq 10\,\%$ for the proton flux $R = 1.1 - 2.9$ GV. After the shock-wave propagation, ejecta fill the interplanetary space behind the shock. The FD ends when the ejecta leave the region of interplanetary space occupied by the observation apparatus.

The dependence of recovery time on rigidity can also depend on the interaction between cosmic ray particles and the ejecta. Cane *et al.*, 1994 found that the density of cosmic ray particles inside the ejecta part of ICME increases as it moves away from the Sun. This process can be rigidity-dependent, and this dependence may be more significant for stronger ICMEs. These effects may also be present in slower ICME events. However, in this case, the time scale of the effect is probably shorter than a day, below the threshold of statistical significance for the PAMELA experiment.

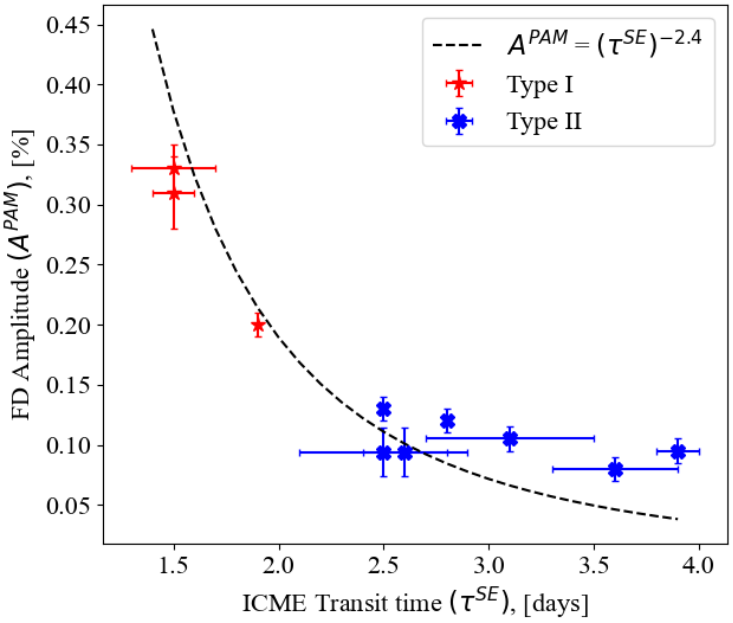

Figure 5. FD amplitudes for the primary proton flux ($R = 1.1-2.9$ GV) and corresponding CMEs transit times τ^{SE}. *Red stars* – Type I FDs, *blue crosses* – Type II FDs, *dashed line* – power law fit of observed dependence.

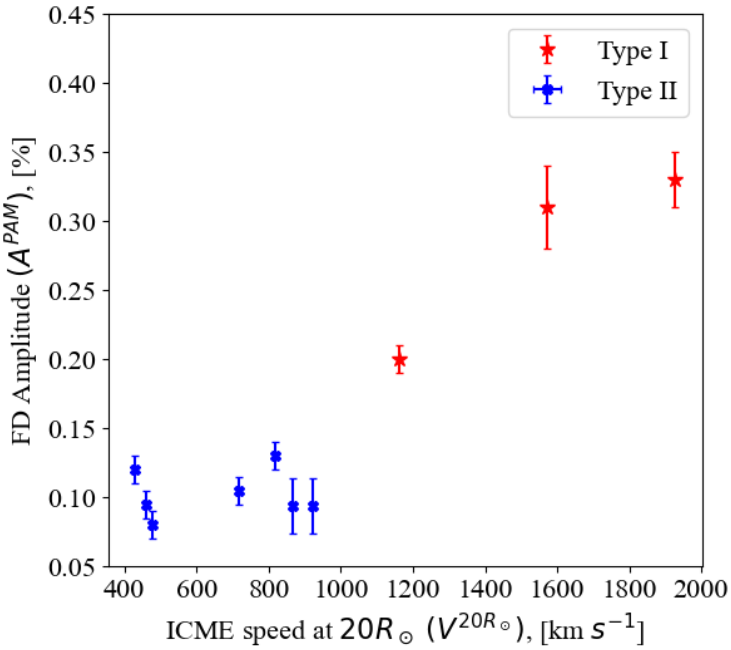

Figure 6. FD amplitudes for the cosmic ray proton fluxes ($R = 1.1-2.9$ GV) measured by the PAMELA experiment and the velocities ($V^{20R_\odot}$) of corresponding ICMEs at a distance of 20 solar radii. The classification of FD events presented in this work is shown as *red stars* for Type I and *blue crosses* for Type II.

5. Conclusions

The measurements of the cosmic ray proton fluxes by the PAMELA experiment allowed a comprehensive study of ten Forbush Decreases that occurred between 2011 and 2013, during the maximum phase of the UC 24. All studied FDs were generated by halo CMEs that created shock-waves in Earth's proximity. The FD recovery time profiles of the cosmic ray proton fluxes measured by the PAMELA experiment for seven rigidity intervals (see Table 2) were obtained and fitted with an exponential function. From the resulting recovery times it appeared that the FDs could be classified in two groups: Type I and Type II. Type I FDs had a significant rigidity dependence of the recovery time and were caused by ICMEs with transit times $\tau^{SE} <$ two days. Their amplitudes were more than 20 % of the mean level of cosmic ray proton flux in the rigidity range 1.1 – 2.9 GV. Type II FDs had no clear recovery time dependence and smaller amplitudes, less than 20 %. The ICMEs causing these FDs had transit times longer than two days.

Two possible explanations for these effects were considered. High-rigidity particles are less affected by the dissipated shock-wave than low energetic ones thus reducing the duration of the recovery phase. Similarly, the ejecta material should affect cosmic rays differently depending on their rigidity, impacting more low-rigidity particles.

Funding Event selection and data analysis have been performed with the support of the Russian Science Foundation, project no. 20-72-10170. Theoretical treatment of obtained results was supported by the Ministry of Science and Higher Education of the Russian Federation, project "Fundamental problems of cosmic rays and dark matter", no. 0723-2020-0040.

Data Availability Data available within the article.

Declarations

Conflict of interest The authors declare that they have no conflicts of interest.

References

Adriani, O., Barbarino, G.C., Bazilevskaya, G.A., Bellotti, R., Boezio, M., Bogomolov, E.A., Bongi, M., Bonvicini, V., Bottai, S., Bruno, A., Cafagna, F., Campana, D., Carbone, R., Carlson, P., Casolino, M., Castellini, G., De Pascale, M.P., De Santis, C., De Simone, N., Di Felice, V., Formato, V., Galper, A.M., Giaccari, U., Karelin, A.V., Kheymits, M.D., Koldashov, S.V., Koldobskiy, S., Krut'kov, S.Y., Kvashnin, A.N., Leonov, A., Malakhov, V., Marcelli, L., Martucci, M., Mayorov, A.G., Menn, W., Mikhailov, V.V., Mocchiutti, E., Monaco, A., Mori, N., Munini, R., Nikonov, N., Osteria, G., Papini, P., Pearce, M., Picozza, P., Pizzolotto, C., Ricci, M., Ricciarini, S.B., Rossetto, L., Sarkar, R., Simon, M., Sparvoli, R., Spillantini, P., Stozhkov, Y.I., Vacchi, A., Vannuccini, E., Vasilyev, G.I., Voronov, S.A., Wu, J., Yurkin, Y.T., Zampa, G., Zampa, N., Zverev, V.G.: 2014, The PAMELA Mission: Heralding a new era in precision cosmic ray physics. *Phys. Rep.* **544**(4), 323. DOI. ADS.

Adriani, O., Barbarino, G.C., Bazilevskaya, G.A., Bellotti, R., Boezio, M., Bogomolov, E.A., Bongi, M., Bonvicini, V., Bottai, S., Bruno, A., Cafagna, F., Campana, D., Carlson, P., Casolino, M., Castellini, G., de Santis, C., di Felice, V., Galper, A.M., Karelin, A.V., Koldashov, S.V., Koldobskiy, S., Krutkov, S.Y., Kvashnin, A.N., Leonov, A., Malakhov, V., Marcelli, L., Martucci, M., Mayorov, A.G., Menn, W., Mergè, M., Mikhailov, V.V., Mocchiutti, E., Monaco, A., Munini, R., Mori, N., Osteria, G., Panico, B., Papini, P., Pearce, M., Picozza, P., Ricci, M., Ricciarini, S.B., Simon, M., Sparvoli, R., Spillantini,

P., Stozhkov, Y.I., Vacchi, A., Vannuccini, E., Vasilyev, G., Voronov, S.A., Yurkin, Y.T., Zampa, G., Zampa, N.: 2017, Ten years of PAMELA in space. *La Rivista del Nuovo Cimento* **40**(10), 473. DOI. ADS.

Alania, M., Wawrzynczak, A., Sdobnov, V., Kravtsova, M.: 2013, Temporal changes in the rigidity spectrum of forbush decreases based on neutron monitor data. *Solar Phys.* **286**(2), 561. DOI.

Alemanno, F., An, Q., Azzarello, P., Barbato, F.C.T., Bernardini, P., Bi, X., Cai, M., Casilli, E., Catanzani, E., Chang, J., Chen, D., Chen, J., Chen, Z., Cui, M., Cui, T., Cui, Y., Dai, H., Benedittis, A.D., Mitri, I.D., de Palma, F., Deliyergiyev, M., Santo, M.D., Ding, Q., Dong, T., Dong, Z., Donvito, G., Droz, D., Duan, J., Duan, K., D'Urso, D., Fan, R., Fan, Y., Fang, F., Fang, K., Feng, C., Feng, L., Fusco, P., Gao, M., Gargano, F., Gong, K., Gong, Y., Guo, D., Guo, J., Han, S., Hu, Y., Huang, G., Huang, X., Huang, Y., Ionica, M., Jiang, W., Kong, J., Kotenko, A., Kyratzis, D., Li, S., Lei, S., Li, W., Li, W., Li, X., Li, X., Liang, Y., Liu, C., Liu, H., Liu, J., Liu, S., Liu, Y., Loparco, F., Luo, C., Ma, M., Ma, P., Ma, T., Ma, X., Marsella, G., Mazziotta, M.N., Mo, D., Niu, X., Pan, X., Parenti, A., Peng, W., Peng, X., Perrina, C., Qiao, R., Rao, J., Ruina, A., Salinas, M., Shangguan, Z., Shen, W., Shen, Z., Shen, Z., Silveri, L., Song, J., Stolpovskiy, M., Su, H., Su, M., Sun, H., Sun, Z., Surdo, A., Teng, X., Tykhonov, A., Wang, J., Wang, L., Wang, S., Wang, S., Wang, X., Wang, Y., Wang, Y., Wang, Y., Wei, D., Wei, J., Wei, Y., Wu, D., Wu, J., Wu, L., Wu, S.S., Wu, X., Xia, Z., Xu, E., Xu, H., Xu, Z., Xu, Z., Xue, G., Xu, Z., Yang, H., Yang, P., Yang, Y., Yao, H.J., Yu, Y., Yuan, G., Yuan, Q., Yue, C., Zang, J., Zhang, S., Zhang, W., Zhang, Y., Zhang, Y., Zhang, Y., Zhang, Y., Zhang, Y., Zhang, Y., Zhang, Z., Zhang, Z., Zhao, C., Zhao, H., Zhao, X., Zhou, C., Zhu, Y., Chen, W., Feng, L., Luo, X., Zhu, C.: 2021, Observations of forbush decreases of cosmic-ray electrons and positrons with the dark matter particle explorer. *Astrophys. J. Lett.* **920**(2), L43. DOI.

Arunbabu, K., Antia, H., Dugad, S., Gupta, S., Hayashi, Y., Kawakami, S., Mohanty, P., Oshima, A., Subramanian, P.: 2015, How are forbush decreases related to interplanetary magnetic field enhancements? *Astron. Astrophys.* **580**, A41. DOI.

Belov, A., Eroshenko, E., Oleneva, V., Struminsky, A., Yanke, V.: 2001, What determines the magnitude of forbush decreases? *Adv. Space Res.* **27**(3), 625. DOI.

Cane, H.V.: 2000, Coronal mass ejections and forbush decreases. *Space Sci. Rev.* **93**, 55. DOI.

Cane, H.V., Richardson, I., Von Rosenvinge, T., Wibberenz, G.: 1994, Cosmic ray decreases and shock structure: A multispacecraft study. *J. Geophys. Res. Space Phys.* **99**(A11), 21429. DOI.

Dumbović, M., Vršnak, B., Čalogović, J., Župan, R.: 2012, Cosmic ray modulation by different types of solar wind disturbances. *Astron. Astrophys.* **538**, A28. DOI.

Forbush, S.E.: 1937, On the effects in cosmic-ray intensity observed during the recent magnetic storm. *Phys. Rev.* **51**(12), 1108. DOI. ADS.

Gopalswamy, N.: 2006, Properties of interplanetary coronal mass ejections. *Space Sci. Rev.* **124**(1), 145. DOI.

Lagoida, I., Voronov, S., Mikhailov, V.: 2019, Forbush decreases in the fluxes of galactic cosmic rays, according to the pamela experiment. *Bull. Russ. Acad. of Sci. Phys.* **83**(8), 971. DOI.

Lockwood, J., Webber, W., Jokipii, J.: 1986, Characteristic recovery times of forbush-type decreases in the cosmic radiation: 1. observations at earth at different energies. *J. Geophys. Res. Space Phys.* **91**(A3), 2851. DOI.

Lockwood, J.A.: 1971, Forbush decreases in the cosmic radiation. *Space Sci. Rev.* **12**(5), 658. DOI. ADS.

Martucci, M., Munini, R., Boezio, M., Di Felice, V., Adriani, O., Barbarino, G.C., Bazilevskaya, G.A., Bellotti, R., Bongi, M., Bonvicini, V., Bottai, S., Bruno, A., Cafagna, F., Campana, D., Carlson, P., Casolino, M., Castellini, G., De Santis, C., Galper, A.M., Karelin, A.V., Koldashov, S.V., Koldobskiy, S., Krutkov, S.Y., Kvashnin, A.N., Leonov, A., Malakhov, V., Marcelli, L., Marcelli, N., Mayorov, A.G., Menn, W., Mergè, M., Mikhailov, V.V., Mocchiutti, E., Monaco, A., Mori, N., Osteria, G., Panico, B., Papini, P., Pearce, M., Picozza, P., Ricci, M., Ricciarini, S.B., Simon, M., Sparvoli, R., Spillantini, P., Stozhkov, Y.I., Vacchi, A., Vannuccini, E., Vasilyev, G., Voronov, S.A., Yurkin, Y.T., Zampa, G., Zampa, N., Potgieter, M.S., Raath, J.L.: 2018, Proton Fluxes Measured by the PAMELA Experiment from the Minimum to the Maximum Solar Activity for Solar Cycle 24. *Astrophys. J. Lett.* **854**(1), L2. DOI. ADS.

Munini, R., Boezio, M., Bruno, A., Christian, E.C., de Nolfo, G.A., Di Felice, V., Martucci, M., Merge', M., Richardson, I.G., Ryan, J.M., Stochaj, S., Adriani, O., Barbarino, G.C., Bazilevskaya, G.A., Bellotti, R., Bongi, M., Bonvicini, V., Bottai, S., Cafagna, F., Campana,

D., Carlson, P., Casolino, M., Castellini, G., De Santis, C., Galper, A.M., Karelin, A.V., Koldashov, S.V., Koldobskiy, S., Krutkov, S.Y., Kvashnin, A.N., Leonov, A., Malakhov, V., Marcelli, L., Mayorov, A.G., Menn, W., Mikhailov, V.V., Mocchiutti, E., Monaco, A., Mori, N., Osteria, G., Panico, B., Papini, P., Pearce, M., Picozza, P., Ricci, M., Ricciarini, S.B., Simon, M., Sparvoli, R., Spillantini, P., Stozhkov, Y.I., Vacchi, A., Vannuccini, E., Vasilyev, G., Voronov, S.A., Yurkin, Y.T., Zampa, G., Zampa, N., Potgieter, M.S.: 2018, Evidence of Energy and Charge Sign Dependence of the Recovery Time for the 2006 December Forbush Event Measured by the PAMELA Experiment. *Astrophys. J.* **853**(1), 76. DOI. ADS.

Nieves-Chinchilla, T., Vourlidas, A., Raymond, J.C., Linton, M., Al-Haddad, N., Savani, N., Szabo, A., Hidalgo, M.A.: 2018, Understanding the internal magnetic field configurations of icmes using more than 20 years of wind observations. *Solar Phys.* **293**(2), 1. DOI.

Penna, R.F., Quillen, A.C.: 2005, Decay of interplanetary coronal mass ejections and forbush decrease recovery times. *J. Geophys. Res. Space Phys.* **110**(A9). DOI.

Picozza, P., Galper, A.M., Castellini, G., Adriani, O., Altamura, F., Ambriola, M., Barbarino, G.C., Basili, A., Bazilevskaja, G.A., Bencardino, R., Boezio, M., Bogomolov, E.A., Bonechi, L., Bongi, M., Bongiorno, L., Bonvicini, V., Cafagna, F., Campana, D., Carlson, P., Casolino, M., de Marzo, C., de Pascale, M.P., de Rosa, G., Fedele, D., Hofverberg, P., Koldashov, S.V., Krutkov, S.Y., Kvashnin, A.N., Lund, J., Lundquist, J., Maksumov, O., Malvezzi, V., Marcelli, L., Menn, W., Mikhailov, V.V., Minori, M., Misin, S., Mocchiutti, E., Morselli, A., Nikonov, N.N., Orsi, S., Osteria, G., Papini, P., Pearce, M., Ricci, M., Ricciarini, S.B., Runtso, M.F., Russo, S., Simon, M., Sparvoli, R., Spillantini, P., Stozhkov, Y.I., Taddei, E., Vacchi, A., Vannuccini, E., Voronov, S.A., Yurkin, Y.T., Zampa, G., Zampa, N., Zverev, V.G.: 2007, PAMELA A payload for antimatter matter exploration and light-nuclei astrophysics. *Astropart. Phys.* **27**(4), 296. DOI. ADS.

Richardson, I., Cane, H.: 1995, Regions of abnormally low proton temperature in the solar wind (1965–1991) and their association with ejecta. *J. Geophys. Res. Space Phys.* **100**(A12), 23397. DOI.

Usoskin, I., Braun, I., Gladysheva, O., Hörandel, J., Jämsén, T., Kovaltsov, G., Starodubtsev, S.: 2008, Forbush decreases of cosmic rays: Energy dependence of the recovery phase. *J. Geophys. Res. Space Phys.* **113**(A7). DOI.

Wibberenz, G., Le Roux, J., Potgieter, M., Bieber, J.: 1998, Transient effects and disturbed conditions. *Space Sci. Rev.* **83**(1), 309. DOI. ADS.

Zhao, L.-L., Zhang, H.: 2016, Transient galactic cosmic-ray modulation during solar cycle 24: A comparative study of two prominent forbush decrease events. *Astrophys. J.* **827**(1), 13. DOI.

Zurbuchen, T.H., Richardson, I.G.: 2006, In-situ solar wind and magnetic field signatures of interplanetary coronal mass ejections. *Space Sci. Rev.*, 31. DOI.